Available online at www.sciencedirect.com

SciVerse ScienceDirect

Ceramics International 39 (2013) 6509–6516

CERAMICS INTERNATIONAL

www.elsevier.com/locate/ceramint

Mechanical and histological evaluation of a plasma sprayed hydroxyapatite coating on a titanium bond coat

Yung-Chin Yang[a,*], Chyun-Yu Yang[b]

[a]Institute of Materials Science and Engineering, National Taipei University of Technology, Taipei 106, Taiwan, ROC
[b]Department of Orthopedics, National Cheng Kung University Medical Center, Tainan, Taiwan, ROC

Received 19 November 2012; received in revised form 26 January 2013; accepted 26 January 2013
Available online 4 February 2013

Abstract

To improve the biological stability of hydroxyapatite-coated implants, the use of an appropriate commercial pure titanium bond coat (CP-Ti) is an effective method for significant improvement in the interface bonding and stress reduction of the plasma-sprayed HA coating and Ti-alloy system. The purpose of this study was to determine the effect of plasma-sprayed CP-Ti on the in vivo properties of the HA coating on Ti6Al4V. According to the experimental results, samples with an HA coating on the CP-Ti (Ti-HA coating) display a lower and ineffective residual stress than samples without the bond coat. The CP-Ti provides a very rough surface and results in a higher adhesive strength between the HA and CP-Ti. In the *in vivo* test, after the intramedullary implantation, the histological observation showed the apposition of the new bone tissue directly onto the HA coating. The shear strength between the bone and the Ti-HA coating was higher than that without CP-Ti after 12 weeks of implantation (5.15 vs. 1.41 MPa). The failure mode analysis showed the failure mainly occurring at the surrounding bone, with some failure at the HA/CP-Ti interface. The excellent bio-durability and mechanical properties of the HA coating in this study contributed to the reduction of the compressive residual stress in the HA coating and to the enhancement of interface adhesive strength by introducing the commercial pure titanium bond coat.

Keywords: Plasma spray; Residual stress; Hydroxyapatite; Bond coat

1. Introduction

During the clinical use of hydroxyapatite-coated implants, failures may occur at the coating-substrate interface [1,2]. In a similar *in vivo* test, mechanical failure was noted to occur at the same location as in the push-out tests [3–5]. One of the reasons hydroxyapatite coating delaminates from the metal implant is an insufficient adhesion between the ceramic material and the substrate [1]. In addition to an HA coating degradation, in-plane compressive stress existing at the implant surface might induce a through-thickness tensile stress that is likely to weaken the adhesion between the HA coating and the Ti substrate. An oxide layer under compression on a metallic substrate (with a semi-infinite plate geometry) will buckle if the compressive stress reaches a critical value [6]

$$\sigma_{\text{compress}} \geq \sigma_{\text{buckle}} = \frac{kE_{\text{ox}}}{12(1-v_{\text{ox}}^2)}\left(\frac{t}{c}\right)^2 \quad (1)$$

provided a separation (radius c) pre-exists at the oxide–substrate interface (k is a constant of ≈ 14.7). In Eq. (1), E_{ox} and v_{ox} are Young's modulus and Poisson's ratio of the oxide coating, respectively, and t is the thickness of the oxide coating. Therefore, the preexisting residual stress or strain in the coating deposited on the stem may be added to the subjected compressive strain in the stem or coating [7], affecting the coating's performance. The industrial use of the plasma-sprayed coating is sometimes limited by the stresses generated during deposition [8]. Different stress states occur during various stages of the deposition process. During the initial contact of the sprayed molten materials with the substrate, a quenching stress, always tensile, is induced within the coating [9,10]. During the cooling stage, a thermal stress gradient appears in the

*Corresponding author. Tel.: +886 921510383.
E-mail address: ycyang@ntut.edu.tw (Y.-C. Yang).

0272-8842/$ - see front matter © 2013 Elsevier Ltd and Techna Group S.r.l. All rights reserved.
http://dx.doi.org/10.1016/j.ceramint.2013.01.083

through-section of the coating/substrate system. Residual stress in the coating may vary with the coating thickness [6–11], spraying parameter [12–14], and temperature of the substrate [8,9].

To control and reduce thermal residual strain is always an important concern in the study of the spraying process. The substrate temperature and the simultaneous cooling are considered two main factors that manage residual stress in the thermal spray coating. In the previous study [12], to examine the influence of residual stress on bonding strength in HA coatings, several HA coatings with a range of bonding strengths and residual stresses in the materials were designed by varying the substrate temperatures and cooling conditions. We found that the residual stress of specimens without cooling during spraying was significantly higher than those prepared with cooling media, with the additional residual stress a result of the higher substrate temperature measured during plasma spraying. The same results were also found in substrates with the initial temperatures varied. The HA coating on the pre-heated substrate (250 °C) had the highest compressive residual stress. In contrast, for an initial substrate temperature of 25 °C (without pre-heating), the lowest compressive residual stress was obtained. Based on these observations, this study investigates replacing the adjustment of the substrate temperature with employing a bond coat to modulate the thermal mismatch between the HA coating and the Ti-substrate.

In this investigation, hydroxyapatite powders have been sprayed on the surface of a commercial pure titanium bond coat (CP-Ti), and an intramedullary implant model was developed to evaluate the mechanical and histological responses between cancellous bone and the coatings. The HA coated implant without CP-Ti (P-HA) was also investigated for comparison.

2. Materials and methods

2.1. Fabrication of implants

In this study, cylindrical rods of Ti–6Al–4V alloy were used as substrates. Medical-grade high purity hydroxyapatite powder (Amdry 6021, Sulzer Metco Inc.) conforming to ASTM designation F-1185 with powder sizes ranging from 45 to 125 μm was used in the coating process (Fig. 1a). Commercial pure Ti powder (AMDRY 9182, 99.4%, $\phi = 90 \pm 11$ μm) was used as the bond coat material (Fig. 1b). The coating system studied here was the introduction of a plasma-sprayed commercial pure titanium bond coat (CP-Ti) on Ti–6Al–4V substrate prior to the deposition of HA. Plasma spray is a high temperature processing method; to avoid the oxidation of Ti powder during spraying, the spraying deposition must be performed in a vacuum chamber under an Ar atmosphere, i.e., vacuum plasma spray (VPS). The commercial pure Ti powder was first coated by VPS deposition onto the Al_2O_3 grit-blasted substrate of a standard Ti–6Al–4V titanium alloy; then, the HA powder was applied as the top coat onto the surface of intermediate CP-Ti by means of an atmospheric plasma-spaying system (APS). The employed spraying parameters for the HA coating and CP-Ti bond coat using the APS and VPS methods are shown in Table 1. The thickness of the CP-Ti was 100 μm and the total thickness of the two-layer Ti-HA coating was 150 μm. Two types of intramedullary implants were evaluated for comparison: the Ti–6Al–4V substrate with a 100 μm CP-Ti and 50 μm HA top coat (abbr. Ti-HA coating) and the 150 μm HA coating only (abbr. P-HA coating). When measured after plasma spraying, all implants were 4.76 ± 0.04 mm in diameter.

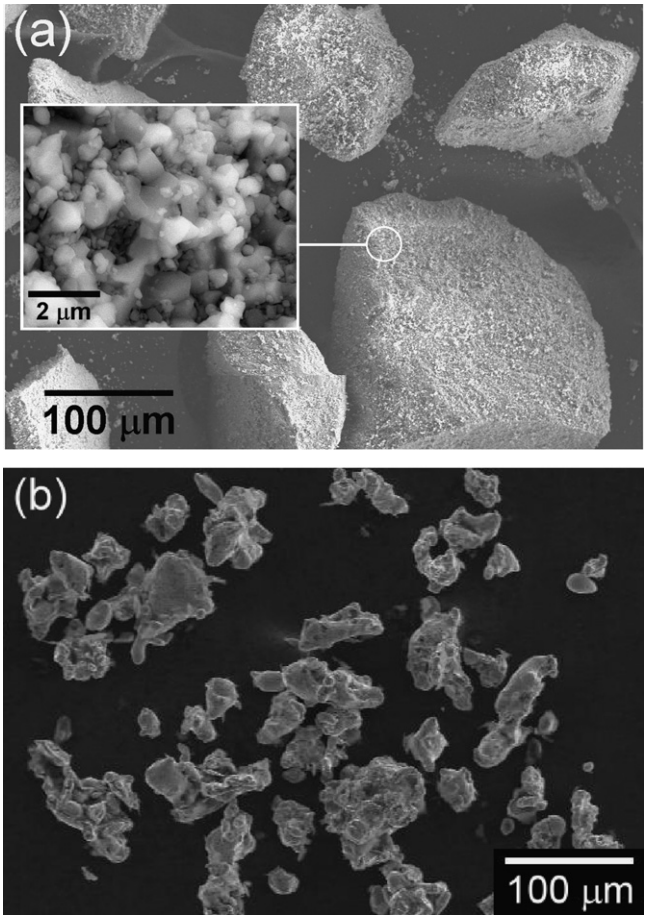

Fig. 1. Surface morphology of (a) HA powder, (b) CP-Ti powder.

Table 1
Spraying parameters employed for preparing HA coating and CP-Ti bond coat.

Parameters	HA coating (APS)	CP-Ti coating (VPS)
Flow rate of primary gas (Ar) (1 min^{-1})	41	50
Flow rate of secondary gas (H_2) (1 min^{-1})	8	6
Flow rate of powder carrier gas (Ar) (1 min^{-1})	3	2
Powder feed rate (g min^{-1})	20	30
Current (A)	660	650
Stand-off distance (cm)	7.5	40
Pressure of chamber (mbar)	–	150

2.2. Surgical techniques

All implants were cleaned by ultrasonically washing in reagent-grade acetone followed by ultrasonically rinsing in distilled water. Dry-heat (120 °C, 8 h) sterilization was used prior to implantation. Under general anesthesia, using sterile techniques, implants were inserted in the distal portion of the canine femora (Fig. 2). To accomplish this, the knee joint was exposed through medial parapatellar arthrotomy after midline skin incision. At the femoral intercondylar notch, a cylindrical hole 4.76 mm in diameter and over 50 mm long was prepared in the medullary cavity with a two-stage power drill at low speed. Next, implants with different coatings were inserted bilaterally into predrilled holes to obtain an interference fit. A total of 12 implants were inserted into the femora of six dogs, where each femur contained one implant. The P-HA implants were inserted into the right femur and the Ti-HA implants were inserted into the left femur. After administering general anesthesia, the three dogs were euthanized after 6 weeks and 12 weeks of implantation.

2.3. Mechanical testing

The bonding strength of the coatings was tested using a standard adhesion test (ASTM C-633, Fig. 3) designed specifically for plasma sprayed coatings. Each test specimen was composed of an assembly of a substrate fixture to which the coating was applied and a loading fixture. Both the substrate and loading fixtures were cylindrical rods of a Ti6Al4V alloy, measuring 2.54 cm in diameter and 5.5 cm in length. Coatings were plasma sprayed on the substrate fixtures. The facings of the loading fixtures were grit-blasted and attached to the surface of the coating using special adhesive glue (METCO EP-15) with an adhesive strength of approximately 60 MPa. The assembly was held perpendicularly and placed in an oven at 180 °C for 2 h. After the bonding glue was cured and hardened, the assembly was loaded in the machine for the measurement of the tensile bonding strength.

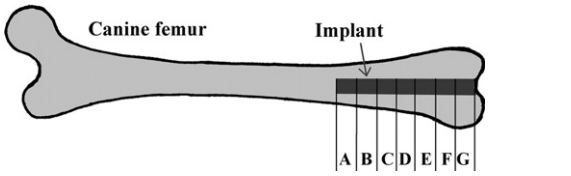

Fig. 2. Schematic representation of the intramedullary implantation model.

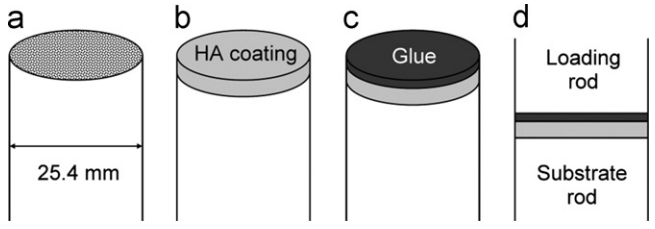

Fig. 3. Representative procedures of ASTM C633 adhesion test: (a) degreased; grit-blasted substrate rod; (b) plasma-sprayed HA coating on substrate rod; (c) glue attached on HA coating and (d) loading rod attached on substrate rod.

Euthanization was performed postoperatively at 6 and 12 weeks of implantation. After euthanization, both ends of the implant were identified and carefully sectioned using a diamond saw to obtain seven implant blocks (marks A–G) of equal length 6 mm (Fig. 2). Block A, C, E and G then were subjected to the push-out test to measure the shear strength at the coating-cancellous bone interface (Fig. 4) while the others (blocks B, D and F) were used for histological evaluations. For the push-out test (Fig. 4), fresh samples were placed in a testing jig and the implants were pushed out from the surrounding bone using an Instron test machine (Instron, UK). The force needed to loosen the implant was determined from the load to displacement curve. The shear strength at the coating/cancellous bone interface was calculated by dividing the maximum push-out force by the total implant area in contact with the cancellous bone: $S=F/\pi DL$, where S is the shear strength, D is the diameter of the implant (4.76 mm), and L is the length of the implant block (6 mm). After the push-out test, a failure mode analysis was performed using SEM on the fractographs of implants.

2.4. Characteristics of the coatings

The melting characteristics of the coatings were assessed from the surface morphology of the coatings by scanning electron microscopy (SEM) (JEOL, JSMr 840). The thicknesses and microstructures of the coatings were also examined cross-sectionally by the use of backscattered electron imaging (BEI) in an SEM. In addition, the surface roughness of the HA coating, CP-Ti and Ti-substrate were determined using a surface roughness meter (Surfcorder SE-30H, Kosaka Laboratory Ltd).

2.5. Histological evaluation

Implant blocks B, D and F were fixed in a 10% formalin buffer and dehydrated in ethyl alcohol solutions varying from 70% to 100%. The blocks were then mounted by the light-curing resin (EXAKT, Technovit 7200 VLC, Heraeus Kulzer Gmbh, Germany). Each undecalcified block was sectioned perpendicularly to the longitudinal axis of the implant into three thin slices (approximately 150 μm) with

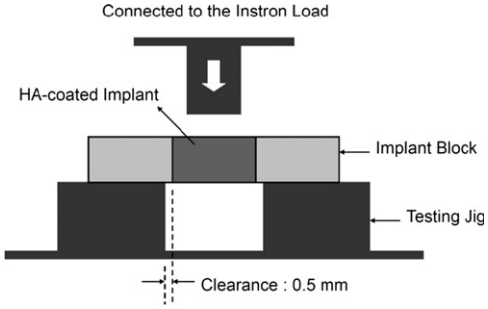

Fig. 4. Schematic representation of the push-out test for measuring the shear strength at the HA-cancellous bone interface.

a low-speed diamond saw. The slice was mounted on a glass slide with fast drying glue. After drying, the slice was polished flat with diamond paste (6 μm and 1 μm) and then coated with carbon for backscattered electron imaging (BEI). The image was obtained using a JSM 6300 backscattered scanning electron microscope (SEM). The ability of implants to osseointegrate was addressed as the bone apposition index (AI), defined as: length of direct bone–implant contact/total length of bone–implant interface $\times 100\%$ [15].

2.6. Residual stress measurement

The residual stresses formed in the HA coating were analyzed by x-ray diffractometry using a Siemens D5000 x-ray diffractometer to obtain XRD patterns for the HA coatings. The reflection (621) of hexagonal $Ca_{10}(PO_4)_6(OH)_2$ at approximately $2\theta = 87.32^\circ$ was used in the residual stress analysis. To determine the diffraction angle (2θ) correctly, the peak (532) close to the reflection (621) was used as a reference in the measurement of the 2θ angles. The experimental details of x-ray diffractometry have been described elsewhere [13]. Diffraction measurements were taken at six ψ values ($\psi = 0^\circ$, 18.43°, 26.56°, 30°, 33.21° and 36.27°, where ψ is the angle of tilt for the specimen), corresponding to increments in $\sin^2\psi$. The residual stress (σ) acting in the coating may be calculated by the equation [12–14]

$$\sigma = \frac{(d_i - d_n)/d_n}{\sin^2\psi}\frac{E}{(1+\nu)} \quad (2)$$

where d_n is the crystallographic plane spacing measured at $\psi = 0^\circ$ and d_i is the plane spacing measured at different ψ angles by XRD, ν is Poisson's ratio, and E is Young's modulus. The residual stress (σ) can be obtained from Eq. (2) by measuring the slope of $(d_i - d_n)/d_n/\sin^2\psi$, which was determined from a least square fit of the plot of $(d_i - d_n)/d_n$ against $\sin^2\psi$.

The elastic modulus is a value that combines several characteristics of material. Young's modulus (E) of the HA coating used in relation (2) might be different from that of the bulk materials due to the lower density and the numerous porosity, cracks and impurity phases. Therefore, the value $E = 22.2$ GPa [14] was used instead of the value $E = 110$ GPa for the residual stress calculation. Young's modulus ($E = 22.2$ GPa) was obtained by measuring the free HA coating slice separated from the Ti–6Al–4V substrate using a standard three point bending test [14]. Each measured value of Young's modulus represented an average of three tests. From the test results, the value of Young's modulus was calculated using the relationship [14]

$$E = \frac{PL^3}{4bh^3\delta} \quad (3)$$

where E is Young's modulus value, P is the load, L is the span between supports, b is the specimen width, h is the specimen thickness, and δ is the deflection at midspan. The value ($E = 22.2$ GPa) revealed the complex mechanical properties of the plasma sprayed HA coating as measured by the mechanical test.

3. Results

3.1. Characteristics of the CP-Ti and Ti-HA coating

The microstructures of the CP-Ti and Ti-HA coatings after spraying were examined by SEM. Fig. 5a shows the morphology of CP-Ti to be a completely molten coating with well-flattened droplet powder, with the accumulated droplet powder resulting in a rough surface. Fig. 5b shows the HA coating uniformly sprayed on the CP-Ti without changing the original morphology. A cross section of CP-Ti is shown in Fig. 6a. The Ti powder was well molten and formed a layer structure with a thickness of approximately 100 μm. Due to the molten and interlocked mechanism, we observed excellent bonding between CP-Ti and the substrates, with the CP-Ti still maintaining its surface roughness after application of the HA coating (Fig. 6b). The interface of the CP-Ti/HA revealed good bonding without any cracks or other defects. In Fig. 6b, the HA coating revealed a similar layer structure as the CP-Ti; however, a small amount of extra large powder was partially melted. The incompletely molten core was shown in the layer structure as indicated by the arrow, with the morphology

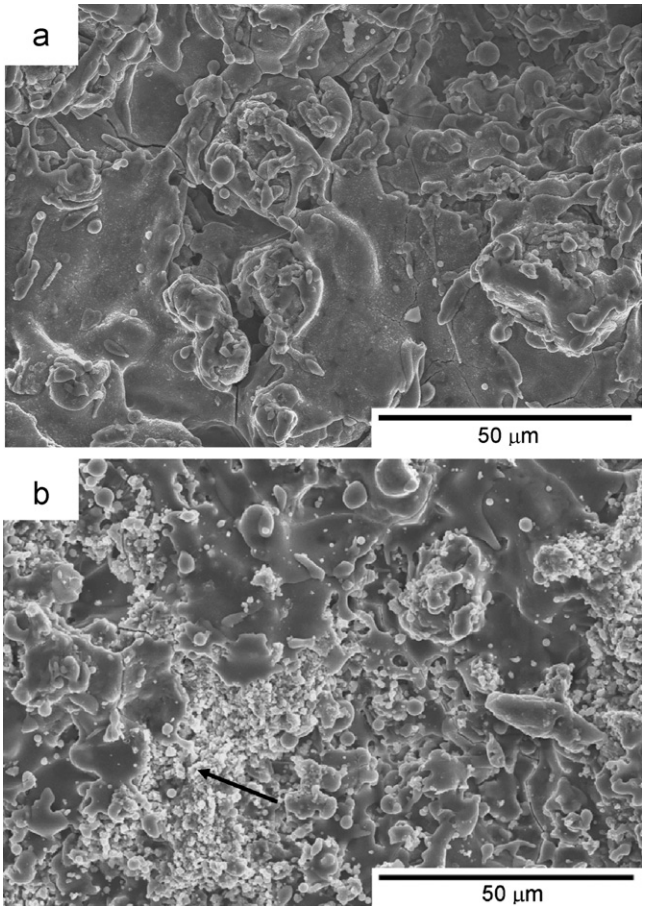

Fig. 5. The surface morphology of the (a) CP-Ti and (b) HA coating on the CP-Ti.

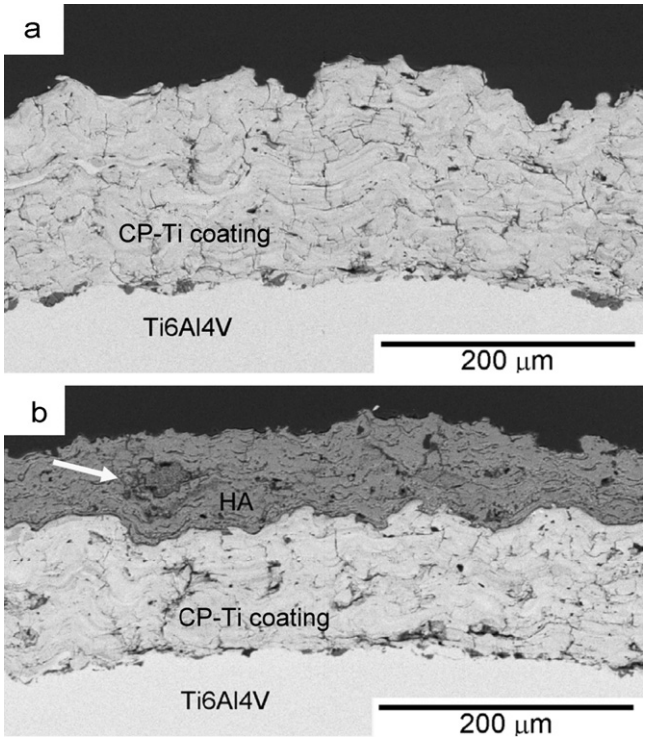

Fig. 6. Cross-sectional BEI images of the (a) CP-Ti and (b) HA coating on the CP-Ti.

of the non-melt core of the HA powder also shown in Fig. 5b and indicated by the arrow.

Fig. 7 displays the diffractograms of the commercial pure Ti powder and CP-Ti coating. The major peak in Fig. 7a matches that of the titanium phase very acceptably (JCPDS no. 05-0682). After the vacuum plasma spraying process, the diffraction pattern of the CP-Ti coating in Fig. 7b is indicative of the titanium phase combined with titanium deuteride ($TiD_{1.5}$, JCPDS no. 78-2216). The mechanism of the titanium deuteride synthesis in the VPS CP-Ti coating is unclear and has never been mentioned in the literature. However, it can be speculated that the source of the deuterium may be the hydrogen ions from the plasma. We will focus on this issue in another work and discuss the mechanism in detail. The diffractograms of the HA powder and HA coating are shown in Fig. 8. The major peak matches the standard HA phase very well ($Ca_{10}(PO_4)_6(OH)_2$, JCPDS no. 9-432). In addition, the HA powder does not show any line-broadening effects and could serve as a standard for 100% crystallinity. Apart from the HA phase, several impurity phases including the α-TCP ($Ca_3(PO_4)_2$), β-TCP, TP ($Ca_4P_2O_9$), and CaO were identified in the HA coating. Moreover, it is noted that the crystallinity of the sprayed HA coating decreased in comparison to that of the HA powder.

The surface roughness (Ra) of the grit-blasted Ti6Al4V substrates is 3.5 μm while after plasma spraying, the surface roughness of CP-Ti is 9.3 μm. This extra-high surface roughness was achieved by introducing plasma sprayed CP-Ti. The bond strength data measured by the

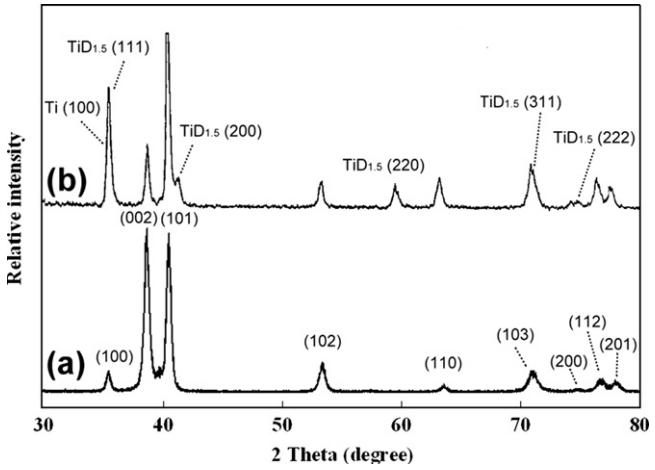

Fig. 7. XRD patterns (Cu Kα) of (a) CP-Ti powder and (b) CP-Ti coating.

adhesion test according to ASTM C633-79 were shown in Table 2. As shown in Table 2, the CP-Ti bond coat displayed approximately twice the bonding strength of P-HA. The Ti-HA exhibited an obviously higher bonding strength than P-HA (38.4 MPa *vs.* 25.6 MPa).

To further study the residual stress of the coatings, measurements of $\Delta d/d$ vs. $\sin^2\psi$ (i.e., $(d_i - d_n)/d_n$ vs. $\sin^2\psi$) for P-HA and Ti-HA acquired by using the XRD method are shown in Fig. 9. The calculated residual stress values with respect to the spraying direction are shown in Table 2. The HA coating with CP-Ti displayed a lower compressive residual stress than the HA coating alone. This means that the porous Ti bond coat could moderate the thermal expansion mismatch between the HA coating and the Ti-alloy substrate.

The bonding strength of a coating is a manifestation of the adhesive and cohesive strength of a coating [16]. Because the porosity with value around 6.5% [16] of the HA coatings are the same, this factor should not be considered further. The adhesive strength between the coating and the substrate is affected by the residual stress and surface roughness. Introducing the CP-Ti bond coat not only provided a rougher interface for the HA coating but also reduced the compressive residual stress of the HA coating. Both of these factors increased the adhesive strength between the coating and the substrate, and, therefore, the Ti-HA displayed a higher bonding strength than P-HA [16].

3.2. Histological evaluation

The surgery was well tolerated by the dogs. At harvesting, there were no signs of infection or metallic staining around the implants, which were firmly fixed to the surrounding bone. The comparison of Ti-HA implants after 6 weeks and 12 weeks implantation was investigated as seen in Fig. 10. The direct cancellous bone-to-HA contact (osseointegration) was observed partly at the interface, and no intervening fibrous tissue was seen. The bone apposition index of the sample at 6 weeks of implantation is approximately 55, which

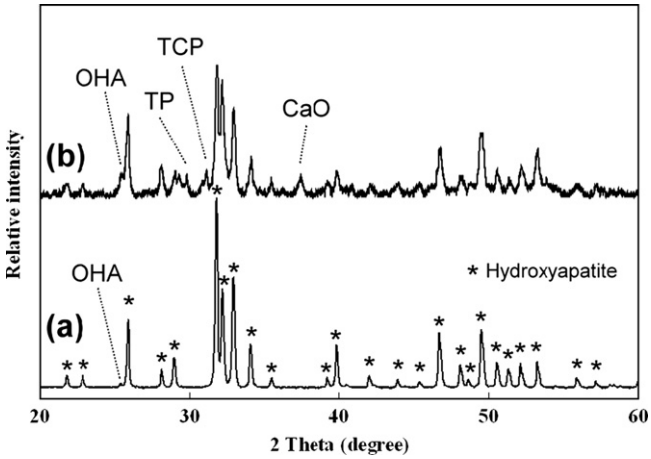

Fig. 8. XRD patterns (Cu Kα) of the (a) HA powder and (b) HA coating.

Table 2
Results of mechanical measurement in various coatings.

(MPa)	Coatings		
	CP-Ti	Ti-HA	P-HA
Residual stress[a]	–	−31.8	−44.2
Bonding strength[b]	49.17 ± 2.57	38.4 ± 3.02	25.6 ± 2.57
Shear strength[c]	–	5.15 ± 1.5 (12 weeks) 4.27 ± 1.24 (6 weeks)	2.38 ± 0.11 (12 weeks) 1.72 ± 0.12 (6 weeks)

CP-Ti: titanium coating on Ti substrate, Ti-HA: HA coating on CP-Ti, P-HA: HA coating on Ti substrate.
[a]Negative value means a compressive state.
[b]Each value is the average of five tests; values are given as the mean ± SD.
[c]Values are given as the mean ± SD; each value is the average of four or three tests.

is lower than the 83% observed at 12 weeks of implantation. After 12 weeks of implantation, more new bone was intimately apposed to the HA coatings (Fig. 10b). The results of the P-HA implant were analogous to those of the Ti-HA implant. The phenomenon of osseointegration was apparent for both periods.

3.3. Shear strength at coating-cancellous bone interface

The interface shear strength data obtained from the push-out test are summarized in Table 2. It was clearly noted that the mean shear strength data of the Ti-HA implants were obviously higher than that of the P-HA implants at each implant period (6 and 12 weeks). The Ti-HA implants at 6 weeks implantation had a shear strength of 4.27 ± 1.24 MPa, and the same coating at 12 weeks implantation had the higher data of 5.15 ± 1.5 MPa. These data may be compared to the P-HA implant, which displayed fairly low shear strengths of 1.72 ± 0.12 MPa and 2.38 ± 0.11 MPa after an insertion of 6 and 12 weeks.

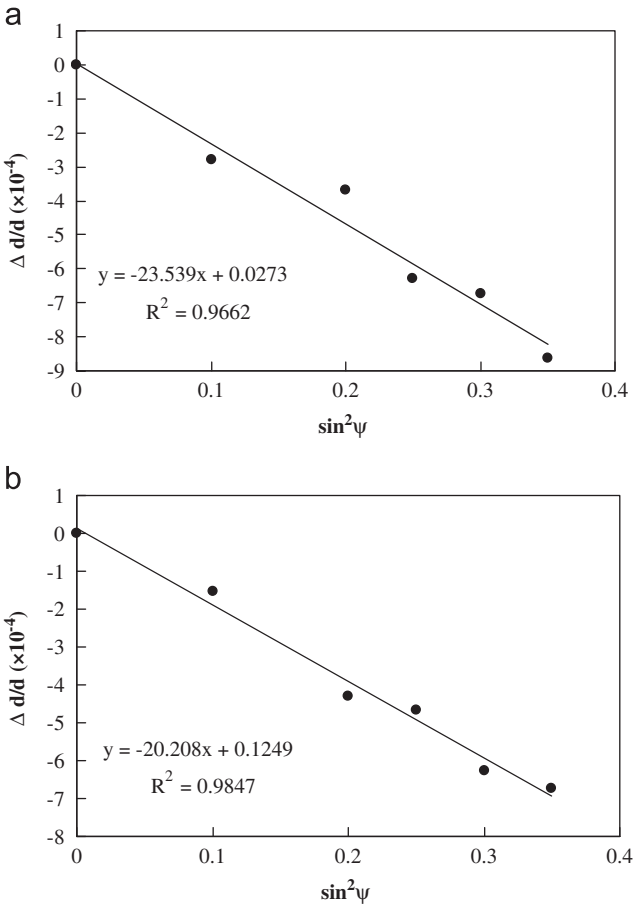

Fig. 9. Plot of $\Delta d/d$ versus $\sin^2\psi$ of the (a) P-HA coating, (b) Ti-HA coating.

3.4. Failure mode analysis

The gross view of the failure site after the push-out test of the Ti-HA and P-HA is shown in Fig. 11, with a different failure mode found in each respective implant. For the Ti-HA implant, most of the surface of the Ti-HA implant was covered with the broken bones, which means that the failure occurred in the cancellous bone near the HA/bone interface (Fig. 11a). From this, we can say that the bonding between the HA coating and the cancellous bone was stronger than the strength of the bone itself. For P-HA implant, the data in Fig. 11b revealed the typical failure seen after the push-out test. As shown in Fig. 11b, some failure occurred inside the HA coating layer and some occurred in the HA/Ti-substrate interface. As can be inferred from the two failure modes, the bonding strength between the HA and the bone should be higher than the bone strength and the bonding strength between the HA and the Ti-substrate interface. Furthermore, by comparing the failure mode of these two implants, we can deduce that the CP-Ti bond coat provided strong bonding both to the HA top coat and to the Ti-substrate.

4. Discussion

There are several commonly used methods for stress determination in coatings: mathematical modeling (analytical

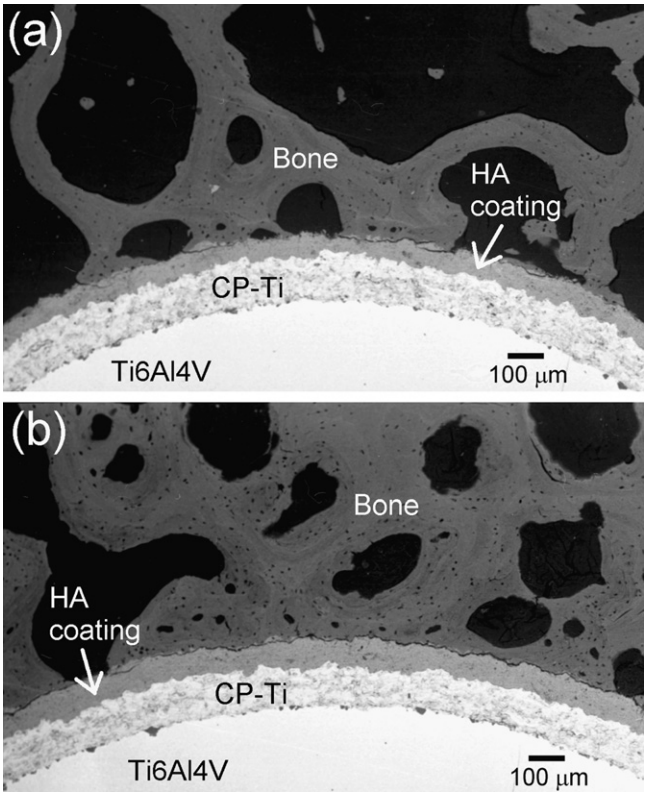

Fig. 10. Histological appearance at the cancellous bone and Ti-HA interface at (a) 6 weeks implantation and (b) 12 weeks implantation.

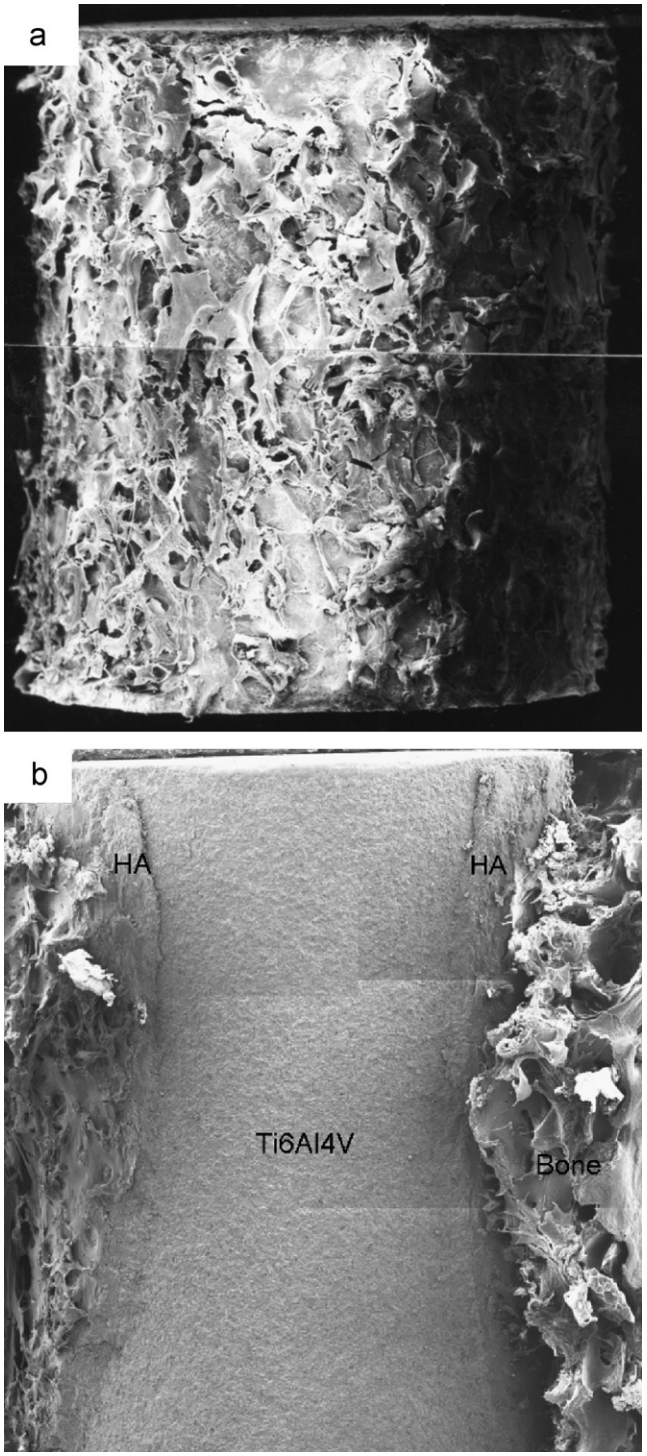

Fig. 11. The gross view of a typical (a)Ti-HA and (b)P-HA implants after the push-out test.

or numerical), materials removal techniques (hole drilling, layer removal), curvature methods (curvature in situ, deflection, or strain measurement), and diffraction methods (X-ray, neutron or Raman). Each technique has certain advantages and limitations [17–18]. The diffraction method is the most popular method for direct measurement of residual stresses via monitoring the shift of selected X-ray diffraction peaks [19]. Due to the limited penetration depth of X-rays, one alternative to XRD is the use of neutrons. However, the scattering intensities of neutron diffraction tend to be relatively low, and, therefore, it is very difficult to obtain sufficient data in a reasonable time from small volumes, such as those of interest in coatings. The diffraction method also includes Raman spectroscopy, which has been used to measure stresses in chemical vapor deposition (CVD) films, but has not been widely applied to thermally sprayed coatings. Therefore, the x-ray diffraction technique for residual stress measurement is a convenient and reliable method to investigate the stress state of the thermal spray coating system.

It is generally believed that the failure mode at the implant–bone interface influences the results of mechanical evaluations and the long-term stability of the implants. In our previous study [12], the residual stress in the coating tends to increase the tendency of the coating to fail adhesively at the HA/Ti-substrate interface. The rough surface could enhance the adhesive strength of the HA/Ti-substrate interface. For the Ti-HA coating evaluated in this study, the failure mode, which fractured inside the bone, apparently indicated that the commercial pure Ti bond coat (CP-Ti) provided strong fixation to the HA top coat. This was attributed to the fairly rough surface of the plasma sprayed CP-Ti, which provided higher mechanical bonding with the HA coating than the grit-blasted Ti-alloy substrate. Additionally, the lower compressive residual stress in HA coating achieved by introducing CP-Ti was also an important factor. Conversely, the P-HA implant

showed a lower shear strength, which could be attributed to insufficient adhesive strength of the HA/Ti-substrate interface. Fig. 11b displayed the clear image of HA coating fractured after shear strength test.

According to the work of Otani et al. [7], they obtained a strain distribution of 0.091% to 0.084% in the proximal femur with the Ti6Al4V component under 2000 N axial loads [7]. The pre-existing residual compressive strains in the HA coating even after 4 weeks of immersion in SBF evaluated in our previous work [20] are of comparable or larger magnitude than the loading strain on the HAC as inferred from the study of Otani et al. Therefore, the residual strain existing in the HAC might be a significant factor for the durability of the coating on an artificial implant as implied by Eq. (1) [6]. Residual stress in the compressive state of plasma-sprayed ceramic coatings on metal substrates tends to delaminate the coatings from the substrate as per Eq. (1) [6]. The stress is reasonably suspected to act adversely on the bonding at the HA coating and titanium substrate interface, where the coating on implants fails mechanically in the present study. This statement was also supported by Rakngarm's work [21]. In their works, the plasma spraying of a hydroxyapatite top coat on titanium bond coat was examined under cyclic fatigue tests. A significant reduction in debonding and cracking in the specimen with Ti bond coat would result from the reduction of residual stress due to the intermediate thermal expansion coefficient of the bond coat.

To improve the durability of HA coatings, the cohesive and adhesive strength of HA coatings should be improved. This can be achieved by increasing the spraying power and using the smaller HA powder, etc. to obtain the densest coating for increased cohesive strength. In addition, based on the results of this study, both an increase of the interface roughness and a decrease in the residual stress of the coating are achieved by introducing the CP-Ti bond coat between the HA coating and the Ti substrate. This promotes adhesive strength between the HA coating and the under interface, improving the durability of implants in bone.

5. Conclusions

Ti-HA coating showed higher shear strength than the P-HA coating in this intramedullary model. The CP-Ti bond coat can improve the bonding strength of the HA coated implants. From the fractography, the HA/Ti-substrate interface displayed the weakest linkage. The excellent bio-durability and mechanical properties of the HA coating in this study contributed to the reduction of the compressive residual stress in the HA coating and the enhancement of the interface adhesive strength by introducing the commercial pure titanium bond coat.

References

[1] W. Thomas, C.T. Rudolph, Z. Richard, T. James, Hydroxyapatite coated femoral stems, Journal of Bone and Joint Surgery (American Volume) 73A (1991) 1452–1493.

[2] W.P. Hu, K.A. Lai, C.Y. Lin, C.Y. Yang, G.L. Chang, Retrieval study on hydroxyapatite-coated acetabular cups, in: Proceedings of the Northeast Conference IEEE 28th Annual Northeast Bioengineering Conference. Piscataway, NJ, 2002 pp. 5–6.

[3] J.M. Spivak, J.L. Ricci, N.C. Blumenthal, H. Alexander, A new canine model to evaluate the biological response of intramedullary bone to implant materials and surfaces, Journal of Biomedical Materials Research 24 (1990) 1121–1149.

[4] K. Hayashi, T. Mashima, K. Uenoyama, The effect of hydroxyapatite coating on bony ingrowth into grooved titanium implants, Biomaterials 20 (1999) 111–119.

[5] T. Inadome, K. Hayashi, Y. Nakashima, H. Tsumura, Y. Sugioka, Comparison of bone–implant interface shear strength of hydroxyapatite-coated and alumina-coated metal implants, Journal of Biomedical Materials Research 29 (1995) 19–24.

[6] A.G. Evans, G.B. Crumley, R.E. Demaray, On the mechanical behavior of brittle coatings and layers, Oxidation of Metals 20 (1983) 196–216.

[7] T. Otani, L.A. Whiteside, S.E. White, Strain distribution in the proximal femur with flexible composite metallic femoral components under axial and torsional loads, Journal of Biomedical Materials Research 27 (1993) 575–585.

[8] S. Paolom, L. Matteo, B. Luca, Residual stresses in plasma sprayed partially stabilised zirconia TBCs: influence of the deposition temperature, Thin Solid Films 278 (1996) 96–103.

[9] S. Takeuchi, M. Ito, K. Takeda, Modelling of residual stress in plasma-sprayed coatings: efect of substrate temperature, Surface and Coatings Technology 43/44 (1990) 426–435.

[10] S. Kuroda, T.W. Clyne, Quenching stress in thermally sprayed coatings, Thin Solid Films 200 (1991) 49–66.

[11] R. Mevrel, Cyclic oxidation of high-temperature alloys, Materials Science and Technology 3 (1987) 531–535.

[12] Y.C. Yang, E. Chang, Influence of residual stress on bonding strength and fracture of plasma-sprayed hydroxyapatite coatings on Ti–6Al–4V substrate, Biomaterials 22 (2001) 1827–1836.

[13] Y.C. Yang, E. Chang, B.H. Hwang, S.Y. Lee, Biaxial residual stress states of plasma-sprayed hydroxyapatite coatings on titanium alloy substrate, Biomaterials 21 (2000) 1327–1337.

[14] Y.C. Yang, E. Chang, Measurements of residual stresses in plasma-sprayed hydroxyapatite coatings on titanium alloy, Surface and Coatings Technology 190 (2005) 122–131.

[15] T.M. Lee, B.C. Wang, Y.C. Yang, E. Chang, C.Y. Yang, Comparison of plasma-sprayed hydroxyapatite coatings and hydroxyapatite/tricalcium phosphate composite coatings: in vivo study, Journal of Biomedical Materials Research 55 (2001) 360–367.

[16] Y.C. Yang, E. Chang, The bonding of plasma-sprayed hydroxyapatite coatings to titanium: effect of processing, porosity and residual stress, Thin Solid Films 444 (2003) 260–275.

[17] T.W. Clyne, S.C. Gill, Residual stresses in thermal spray coatings and their effect on interfacial adhesion: a review of recent work, Journal of Thermal Spray Technology 5 (1996) 401–418.

[18] O. Kesler, M. Finot, S. Suresh, S. Sampath, Determination of processing-induced stresses and properties of layered and graded coatings: experimental method and results for plasma-sprayed Ni–Al_2O_3, Acta Materialia 45 (1997) 3123–3134.

[19] B.D. Cullity, Elements of X-ray Diffraction, second ed., Addison-Wesley, Reading, MA, 1980, pp. 447–478.

[20] Y.C. Yang, E. Chang, S.Y. Lee, Mechanical properties and Young's modulus of plasmasprayed hydroxyapatite coating on Ti substrate in simulated body fluid, Journal of Biomedical Materials Research 67A (2003) 886–899.

[21] A. Rakngarma, Y. Mutohb, Characterization and fatigue damage of plasma sprayed HAp top coat with Ti and HAp/Ti bond coat layers on commercially pure titanium substrate, Journal of the Mechanical Behavior of Biomedical Materials 2 (2009) 444–453.